

# Transcriptomic Analysis of an In Vitro Murine Model of Ovarian Carcinoma: Functional Similarity to the Human Disease and Identification of Prospective Tumoral Markers and Targets

ULISES URZÚA,<sup>1\*</sup> KATHERINE F. ROBY,<sup>2</sup> LISA M. GANGI,<sup>3</sup> JAMES M. CHERRY,<sup>3</sup>  
JOHN I. POWELL,<sup>4</sup> AND DAVID J. MUNROE<sup>3</sup>

<sup>1</sup>Programa de Biología Celular y Molecular, Instituto de Ciencias Biomédicas,  
Universidad de Chile, Independencia, Santiago, Chile

<sup>2</sup>Department of Anatomy and Cell Biology, University of Kansas Medical Center,  
Kansas City, Kansas

<sup>3</sup>Laboratory of Molecular Technology, SAIC-Frederick, Inc.,  
National Cancer Institute at Frederick, Frederick, Maryland

<sup>4</sup>Center for Information Technology, National Institutes of Health,  
Bethesda, Maryland

Ovarian cancer is an aggressive disease of poor prognostic when detected at advanced stage. It is widely accepted that the ovarian surface epithelium plays a central role in disease etiology, but little is known about disease progression at the molecular level. To identify genes involved in ovarian tumorigenesis, we carried out a genome-wide transcriptomic analysis of six spontaneously transformed mouse ovarian surface epithelial (MOSE) cell lines, an in vitro model for human ovarian carcinoma. Loess normalization followed by statistical analysis with control of multiple testing resulted in 509 differentially expressed genes using an adjusted  $P$ -value  $\leq 0.05$  as cut-off. The top 20 differentially expressed genes included 10 genes (*Spp1*, *Cyp1b1*, *Btg1*, *Cfh*, *Mt1*, *Mt2*, *Igf1bp5*, *Gstm1*, *Gstm2*, and *Esr1*) implicated in various aspects of ovarian carcinomas, and other 3 genes (*Gsto1*, *Lcn7*, and *Alcam*) associated to breast cancer. Upon functional analysis, the majority of alterations affected genes involved in glutathione metabolism and MAPK signaling pathways. Interestingly, over 20% of the aberrantly expressed genes were related to extracellular components, suggestive of potential markers of disease progression. In addition, we identified the genes *Pura*, *Cnn3*, *Arpc1b*, *Map4k4*, *Tgfb1i4*, and *Crsp2* correlated to in vivo tumorigenic parameters previously reported for these cells. Taken together, our findings support the utility of MOSE cells in studying ovarian cancer biology and as a source of novel diagnostic and therapeutic targets.

Ovarian cancer has remained the most lethal gynecological malignancy in western countries over the last decades. Symptoms are usually vague and unspecific so that early detection is difficult to accomplish. A high number of cases are diagnosed at stages III or IV when local and distant metastases are already present, resulting in a 5-year survival rate of 31% (American Cancer Society, 2004). Because most ovarian tumors arise from the layer of epithelial cells on the ovarian surface, it is widely accepted that repetitive ovulation may play a role in disease etiology (Purdie et al., 2003), but the early events of malignant transformation have not been accurately delineated.

A powerful approach to fill this void is the use of mouse models. Among the recent attempts to recapitulate ovarian cancer in mouse (Vanderhyden et al., 2003), the model of Roby et al. (2000) was obtained by isolation and continuous in vitro culture of mouse ovarian surface epithelial (MOSE) cells. After repeated passages, these cells became spontaneously transformed and tumorigenic. Transformed MOSE cells may contain genetic alterations closely mimicking those generated in situ as result of wound repair triggered proliferative signals after ovulation. Indeed, previous findings of our group support the notion that MOSE cells bear genomic imbalances closely resembling human low malignant potential tumors, serous carcinoma, and ovarian cell lines derived from the latter tumor type (Urzúa et al., 2005). Here we describe a genome-wide transcriptional profile of six clonal tumorigenic MOSE cell lines using

DNA microarray technology. The relevance of this model is supported by the following findings: (1) half of the top 20 aberrantly expressed genes, have been previously implicated in ovarian malignancies; (2) major signal transduction pathways and metabolic alterations of MOSE cells have been also described in human ovarian tumors; (3) over 20% of aberrantly expressed genes are indexed under the GO cellular components "plasma membrane," "extracellular space," and "extracellular matrix," which suggest their evaluation as markers of this malignancy.

## MATERIALS AND METHODS

### Cell lines, RNA isolation, and cDNA labeling

Early passage MOSE cells and MOSE clonal cell lines IF5, 3E3, IC5, ID9, ID3, and IG10 were cultured as described (Roby et al., 2000). Total RNA was extracted from confluent cultures

Contract grant sponsor: Federal Funds from the National Cancer Institute; Contract grant sponsor: National Institutes of Health; Contract grant number: N01-C0-12400.

\*Correspondence to: Ulises Urzúa, Programa de Biología Celular y Molecular, Instituto de Ciencias Biomédicas, Universidad de Chile, Independencia 1027, Santiago, Chile.  
E-mail: uurzua@med.uchile.cl

using Trizol (Invitrogen, Carlsbad, CA). Fluorescent-labeled cDNA was obtained from 8  $\mu\text{g}$  of total RNA using 500 U of SuperScript II (Invitrogen, CA). RT reaction was primed with 1  $\mu\text{g}$  of oligo-dT plus 1  $\mu\text{g}$  of hexamer random primers in the presence of 0.1 mM Cy3 (or Cy5)-dUTP, 0.5 mM of each dATP, dGTP, dCTP, 0.2 mM TTP, 2 U/ $\mu\text{l}$  RNasin, and the SS-II buffer. Reaction was incubated for 2.5 h at 42°C and stopped with EDTA. Template RNA was hydrolyzed with NaOH for 15 min at 65°C. Unincorporated nucleotides were removed by gel filtration with a Bio-Gel P6 column (Biorad, Hercules, CA).

### Microarray hybridization

The NIA-15K mouse cDNA collection (15,261 clones) was spotted onto glass slides using a MicroGrid II arrayer (Biorobotics, Boston, MA). Test and reference labeled samples were combined in approximate Cy3/Cy5 equimolar amounts, and made up to 38  $\mu\text{l}$  solution containing final concentrations of 1  $\mu\text{g}/\mu\text{l}$  mouse COT-1 DNA, 1  $\mu\text{g}/\mu\text{l}$  poly dA, 0.1 % SDS, and  $3.5 \times \text{SSC}$ . This mixture was denatured at 99°C for 3 min, cooled at room temperature, and deposited onto the array surface. Microarrays were incubated at 65°C for 14–18 h. Washes in  $2 \times \text{SSC}$ -0.1% SDS,  $1 \times \text{SSC}$ ,  $0.2 \times \text{SSC}$ , and  $0.05 \times \text{SSC}$  were performed sequentially, 1-min each. Microarrays were quickly dried and scanned at 10- $\mu\text{m}$  resolution in a GenePix 4000B scanner (Axon Instruments, Union City, CA). Voltage was adjusted to obtain maximal signal intensities with minimal saturation. Tiff format images were analyzed with the GenePix Pro III software.

### Data processing and analysis

Biological replicate samples were hybridized against a whole newborn mouse total RNA as reference (replicated dye-swap design). GenePix-Pro results (gpr) files and JPEG images were deposited at the NCI's Microarray Database ("mAdb"; <http://nciarray.nci.nih.gov>). Annotated files were retrieved from mAdb and print-tip loess normalized and scale corrected with DNMA (Vaquerizas et al., 2004; <http://dnmad.bioinfo.cnio.es/>). After eliminate genes found in less than 80% of arrays, the data set size was 11,971 clones. Missing values were estimated with KNN-impute at the GEPAS Preprocessor (Herrero et al., 2003; <http://gepas.bioinfo.cnio.es/cgi-bin/preprocess>). ANOVA, *t*-test, and correlation tests under control of Type I family wise error rate (FWER) were performed with Pomelo (<http://pomelo.bioinfo.cnio.es/>; Herrero et al., 2004). Clustering was done with Sotarray (<http://gepas.bioinfo.cnio.es/cgi-bin/sotarray>) and visualization with SotaTree (<http://gepas.bioinfo.cnio.es/cgi-bin/sotatree>). Gene Ontology (GO) was extracted from GeneCards (<http://bioinfo.weizmann.ac.il/cards/index.shtml>) and from the MGI 3.0 database (<http://www.informatics.jax.org/>). KEGG pathways were accessed at <http://www.genome.jp/kegg/pathway.html>.

### Quantitative PCR validation of microarray results

Primer pairs for the 18S rRNA and for the 3'-mRNA ends of test and control mRNAs were designed with the Assay by Design software (Applied Biosystems, CA). The cDNAs were prepared by reverse transcribing 1  $\mu\text{g}$  of total cellular RNA using the Single-Strand cDNA Synthesis Kit (Roche, Indianapolis, IN) according to manufacturer's protocol. Quantitative-PCR (Q-PCR) assays were conducted in 384-well microtiter plates in 10  $\mu\text{l}$  final volumes. Thermocycling conditions using an Applied Biosystems ABI-7900 SDS machine were as follows: 50°C for 2 min, 95°C for 10 min and 40 cycles of 95°C for 10 sec, and 60°C for 1 min. Quantification of mRNAs was based on  $C_T$  values, which represent the PCR cycle at which an increase in reporter fluorescence above baseline signal can be detected. Normalization was done with the 18S rRNA or the Rps16 mRNA as reference transcript assayed under identical conditions respective to the gene of interest. The  $\Delta\Delta C_{T-\text{Sample}}$  value ( $\Delta\Delta C_{T-\text{Sample}} = \Delta C_{T-\text{Sample}} - \Delta C_{T-\text{Reference}}$ ) was transformed by taking the result of the expression: If  $2^{(-\Delta\Delta C_T)} - 1 > 0$  then the result =  $2^{(-\Delta\Delta C_T)} - 1$  or else the result =  $-1/2^{(-\Delta\Delta C_T)}$ . This calculation converted the range for downregulation from 0–1 to  $-\infty - 0$ , and upregulation from  $1 - \infty$  to  $0 - \infty$ .

## RESULTS

### Microarray data processing pipeline and Q-PCR validation

DNA microarray results are usually subjected to experimental variability so they must be preprocessed before statistical tests. In this report, the data were print-tip loess normalized and scale adjusted. In addition, as statistical analyses consist of simultaneous evaluation of thousands of genes, the probability of producing incorrect test conclusions (false positives and false negatives) may rise markedly. Accordingly, the normalized data was subjected to ANOVA tests with control of the Type I family wise error rate (FWER). A comparison of this method with conventional-direct testing is shown in Supplementary Figure 1B. The output consisted of 509 clones (adjusted  $P < 0.05$ ) that were the subject of functional data mining.

Statistically significant results for clonal MOSE cells were averaged and subtracted from the early passage cells values. *Spp1* and *Mt1* were detected as the highest up and downregulated genes, respectively (see Table 1). Taq-Man Real-time-PCR assays confirmed mRNA levels for both genes in all 7 test and the reference RNA samples. Initial measurements employed the commonly used *Gapd* gene as internal control gene, which

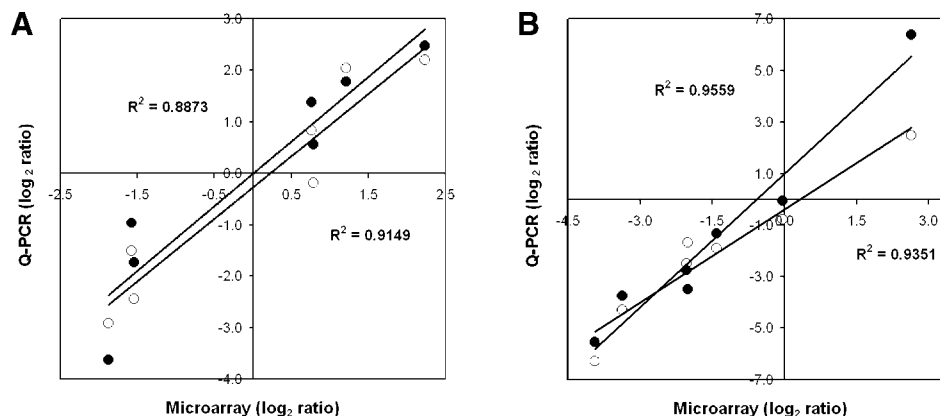


Fig. 1. Quantitative PCR confirmation of microarray data. Correlation between microarray results and Q-PCR results for the expression of *Spp1* (A) and *Mt1* (B). Data represent the average of 6 normalized microarray ratios for the clones H3082C12 (*Spp1*) and H3020C02 (*Mt1*), and the average of duplicate Real-time-PCR assays. Open and

closed circles correspond to Q-PCR results obtained with 18S rRNA and Rps16 mRNA as internal controls, respectively. R<sup>2</sup> values are depicted close to its corresponding tendency line. Raw Q-PCR data are shown in Supplementary Table 1.

TABLE 1. Highest ranking differentially expressed genes in MOSE cells

Gene symbol, description	Mean difference (log <sub>2</sub> scale), adjusted <i>P</i> -value <sup>a</sup>	Reported in cancer <sup>b</sup> (reference)
<b>Upregulated</b>		
<i>Spp1</i> , osteopontin	+3.77, 0.0e0	Ovary (Kim et al., 2002; Brakora et al., 2004)
<i>Cyp1b1</i> , cytochrome P450, family 1, subfamily 1, polypeptide 1	+2.85, 3.1e-3	Ovary (McFadyen et al., 2001)
<i>Nupr1</i> , nuclear protein 1	+2.83, 9.0e-4	Pancreas (Iovanna, 2002)
<i>Gsto1</i> , glutathione S-transferase ω1	+2.52, 0.0e0	Breast (Adam et al., 2002)
<i>Btg1</i> , B-cell translocation gene	+2.41, 0.0e0	Ovary (Bard et al., 2004)
<i>Acsl5</i> , acyl-CoA synthetase long chain 5	+2.35, 0.0e0	Brain (Yamashita et al., 2000)
<i>Perp</i> , TP53 apoptosis effector	+2.23, 6.0e-4	Melanoma (Hildebrandt et al., 2000)
<i>Cfh</i> , complement component factor H	+2.16, 0.0e0	Ovary (Junnikkala et al., 2002)
<i>C3</i> , complement component 3	+2.08, 1.0e-4	Liver (Steel et al., 2003)
<i>Lcn7</i> , lipocalin 7	+2.08, 8.9e-3	Breast (Kobayashi et al., 2001)
<b>Downregulated</b>		
<i>Mt1</i> , metallothionein 1	-4.77, 0.0e0	Ovary (Hengstler et al., 2001)
<i>Mt2</i> , metallothionein 2	-4.66, 0.0e0	Ovary (Hengstler et al., 2001)
<i>Igfbp5</i> , insulin-like growth factor binding protein 5	-3.93, 2.0e-4	Ovary (Hofmann et al., 1994; Kalli and Conover, 2003)
<i>Gstm1</i> , glutathione S-transferase, μ1	-3.32, 0.0e0	Ovary (Matsumoto et al., 1997; Howells et al., 1998)
<i>Alcam</i> , activated leukocyte cell adhesion molecule	-3.08, 1.7e-2	Breast (King et al., 2004)
<i>Gstm2</i> , glutathione S-transferase, μ2	-2.90, 3.5e-2	Ovary (Matsumoto et al., 1997; Howells et al., 1998)
<i>Pcp41l</i> , purkinje cell protein 4-like 1	-2.70, 2.9e-2	n.r. <sup>c</sup>
<i>Uchl1</i> , ubiquitin carboxy-terminal hydrolase L1	-2.54, 1.0e-4	Colorectal (Yamazaki et al., 2002)
<i>Isyna1</i> , myo-inositol 1-P-synthase A1	-2.50, 6.0e-4	n.r. <sup>c</sup>
<i>Esr1</i> , estrogen receptor 1 alpha	-2.47, 0.0e0	Ovary (Hansen et al., 2002)

<sup>a</sup>A multiple ANOVA test with FWER control and 10,000 permutations was conducted for 40 arrays comprising the 6 established clonal MOSE cell lines and the early passage non-tumorigenic MOSE cells. Adjusted *P*-values ≤ 0.05 were obtained for 509 clones. Mean log<sub>2</sub> ratios were calculated for both the early passage cells and for the 6 clonal MOSE cell lines taken as a single group. The difference between these means was ranked from the highest positive (upregulated genes) and from the highest negative (downregulated genes). Further details under Materials and Methods.

<sup>b</sup>PubMed was queried through MedMiner from mAdb employing “gene symbol,” “description,” and “alias” as Gene synonyms and further narrowed with the keywords “tumor” or “cancer” and “ovarian” or “ovary” when corresponded.

<sup>c</sup>To date not reported in connection to cancer or tumor.

ultimately found to be inappropriate as *Gapd* was among the 509 differentially expressed transcripts. We then used the 18S rRNA and the *Rps16* mRNA as internal controls. Interestingly, the latter was chosen from a preliminary screening of genes showing close-to-zero ratios across all samples. Indeed, after data normalization, the three *Rps16* clones showed adjusted *P* = 1.0 and were ranked 9022, 9023, and 9123 among the 11,971 clones that passed filters. As observed in Figure 1, either using the 18S rRNA or the *Rps16* transcript as internal control resulted in good correlation between microarray and Q-PCR results. Importantly, as *Spp1* and *Mt1* were also the top 2 highest variable genes across the 6 MOSE cells (SD 1.55 and 1.51, respectively) the R<sup>2</sup> values shown in Figure 1 further supports the robustness of our Q-PCR platform for array data validation. Raw Ct values are shown in Supplementary Table 1.

### Functional analysis of differentially expressed genes

After removing inconsistent replicates and excluding unknown genes and ESTs, transcribed sequences, and hypothetical proteins, the initial subset of 509 statistically significant transcripts was reduced to 423. The top 20 are shown in Table 1. Half of them (*Spp1*, *Cyp1b1*, *Btg1*, *Cfh*, *Mt1*, *Mt2*, *Igfbp5*, *Gstm1*, *Gstm2*, and *Esr1*) have been involved in various aspects of ovarian cancer, whereas other 3 genes (*Gsto1*, *Lcn7*, *Alcam*) are associated to breast tumors. In contrast, *Pcp41l* and *Isyna1* have not been implicated in cancer to date. *Gsto1*, *Gstm1*, *Gstm2*, *Acsl5*, *Uchl1*, *Isyna1*, and *Cyp1b1* participate in glutathione, fatty acids, protein, phospholipids, and xenobiotics metabolism. *Nupr1*, *Btg1*, and *Esr1* have nuclear localization, and in addition to *Igfbp5* are implicated in cell growth and proliferation. *Igfbp5* plus *Cfh*, *C3*, *Perp*, *Lcn7*, and *Spp1* are associated with the extracellular component and their biological

processes include complement activation, induction of apoptosis, transport, and cell communication.

KEGG analysis of the 423 genes rendered “MAPK signaling” (*Myc*, *Chuk*, *Rasa1*, *Rac1*, *Cacnb3*, *Flnb*, *Hspa5*, and *Hspb1*), “glutathione metabolism” (*Gstm1*, *Gstm2*, *Gstm6*, *Gsto1*, *Idh1*, and *Gpx1*), “glycolysis/gluconeogenesis” (*Pgk1*, *Ldh2*, *Eno1*, *Gapd*, and *Gpi1*), “aminoacyl-tRNA biosynthesis” (*Tars*, *Nars*, *Gars*, *Yars*, and *Farslb*), and “Huntington’s disease” (*Rasa1*, *Gapd*, *Hdh*, and *Calm1*) as the main altered pathways in MOSE cells. Similarly, GO analysis under “biological process-level 3” resulted in 242 genes classified in 21 classes. “Metabolism” was the top-ranked process (139 genes), whereas “cell communication” (49 genes), “response to stimulus” (27), and “death” (11 genes) were among the 7 highest populated terms. These 4 classes were used to tag the whole data subset and run the cluster analysis shown in Figure 2. The upper tree shows early passage MOSE cells (Ep5) clearly discriminated, whereas two secondary branches distinguished MOSE cells ID9, IC5, and ID3 from IG10, IF5, and 3E3. Clusters 3 (95 genes) and 4 (99 genes) discriminated these 2-cell subtypes, whereas clusters 1 (58 genes) and 5 (118 genes) segregated down and upregulated genes in all MOSE cells, respectively. In fact, cluster 5 contained 7 of the top 10 over-expressed mRNAs (see Table 1). In addition, the 27 “cell communication” tagged genes in both clusters were further compared based on “molecular function-level 3.” “Protein binding” was the top ranked class including *Jak2*, *Grid2*, *Cd44*, *Pcdh7*, *Chuk*, *Ptpre*, *Dsg2*, and *Iqgap1* as upregulated genes and *Spnb2*, *Col6a1*, *Calm1*, and *Homer2* as downregulated genes.

GO analysis of the 423 genes under “cellular component-level 4” yielded “plasma membrane” containing 17.3% from the 221 indexed genes. Further analysis under level 3 gave 48 genes in “extracellular space” and “extracellular matrix,” which corresponded to 21.2% of classified genes at that level. From these 48 genes,

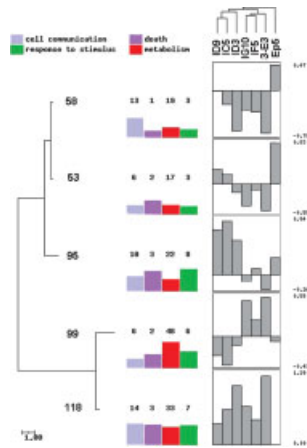


Fig. 2. SOTA clustering of differentially expressed genes. The 509 differentially expressed genes were subjected to cluster analysis. Labeling with the four indicated “biological process-level 3” terms was done with the knowledge filter at GEPAS (<http://gepas.bioinfo.cnio.es/cgi-bin/filtering>). Charts at right show the ratio averages of the total number of genes indicated in branches at left. Euclidean metrics was used for both the vertical and horizontal trees.

34 were over-expressed in any of the clonal MOSE cells respective to the non-tumoral cells. Then, they were ranked from the top upregulated (Table 2). In addition to *Spp1*, *Cyp1b1*, *C3* and *Perp*, which had emerged

previously (Table 1), we identified *Lcn2*, *Mthf2*, *Cdk8*, *Fam3c*, *Nqo3a2*, *Pcdh7*, *Vldlr* and *Emp1* exhibiting over fourfold upregulation. Other 8 genes showed over twofold upregulation including *Itm1* and *Nfe2l1*, which have not been previously involved in cancer, and the gene *2610204L23Rik* with a not known function to date.

**Correlation to in vivo tumorigenesis.**

We used the in vivo tumorigenic data published by Roby et al. (2000) to perform a regression analysis with the complete data set. Results for the highest-ranking correlated genes with “time to death” and “tumor loads” are depicted in Figure 3. The expression of genes *Pura* and *5730469M10Rik*, and genes *BC021790*, *Cnn3* and transcribed sequence (clone ID H3111F06) showed negative and positive correlation to “time to death,” respectively. On the other hand, *Map4k4* and *Crsp2*, as well as *Tgfb1i4*, *Arcp1b* and *2310016E02Rik* showed negative and positive correlation to “tumor loads,” respectively. All adjusted *P*-values using false discovery rate (FDR) control tests at Pomelo (<http://pomelo.bioinfo.cnio.es/>) were under 0.08.

**Mouse-human comparison of ovarian gene expression**

Finally, to address the resemblance of this mouse model to the human situation, we carried out a direct comparison of gene expression profiles between IG10

TABLE 2. Upregulated genes with annotated extracellular localization\*

Gene symbol, description	Highest ratio (log <sub>2</sub> scale) <sup>a</sup> , cell line	Possible role in tumor progression
<i>Spp1</i> , osteopontin	+5.70, 1F5	Regulation of angiogenesis, tumorigenesis and metastasis in various cell types (Coppola et al., 2004)
<i>Cyp1b1</i> , cytochrome P450, family 1, subfamily b, polypeptide 1	+3.72, 1D3	Activation of drugs, environmental mutagens and estrogens (Murray et al., 2001)
<i>C3</i> , complement component 3	+2.91, 3E3	Sublytic doses induce protein kinase C-mediated complement resistance in tumor cells (Donin et al., 2003)
<i>Perp</i> , TP53 apoptosis effector	+2.88, 1G10	Participation in cell type specific p53-mediated apoptosis (Ihrie et al., 2003)
<i>Lcn2</i> , lipocalin 2	+2.73, 3E3	Modulation of estrogen effects on breast epithelium (Seth et al., 2002)
<i>Mthfd2</i> , methenyltetrahydrofolate dehydrogenase	+2.62, 3E3	Supports folate-mediated purine synthesis in tumor cells (Di Pietro et al., 2004)
<i>Cdk8</i> , cyclin-dependent kinase 8	+2.58, 1F5	Indirect control of cell cycle as transcriptional regulator (Sausville, 2002)
<i>Fam3c</i> , family with sequence similarity 3, member C	+2.25, 1C5	Not reported (Pilipenko et al., 2004) <sup>b</sup>
<i>Nqo3a2</i> , NAD(P)H:quinone oxidoreductase type 3, polypeptide A2	+2.22, 3E3	Confers drug resistance through detoxification (Marin et al., 1997)
<i>Pcdh7</i> , protocadherin 7	+2.15, 3E3	Involvement in Ca <sup>2+</sup> mediated-cellular adhesion (Zhang and DuBois, 2001)
<i>Vldlr</i> , very low density lipoprotein receptor	+2.14, 3E3	Regulation of urokinase-mediated tumor cell motility (Webb et al., 1999)
<i>Emp1</i> , epithelial membrane protein 1	+2.13, 1G10	Modulation of c-Myc-mediated cellular proliferation (Ben-Porath et al., 1999)
<i>Fbln2</i> , fibulin 2	+1.63, 1D3	Involvement in fibronectin-mediated cellular adhesion (Gu et al., 2000)
<i>Col6a1</i> , procollagen, type VI, alpha 1	+1.53, 1D9	Confers drug resistance through extracellular matrix remodeling (Sherman-Baust et al., 2003)
<i>Fxyd3</i> , FXDY domain-containing ion transport regulator 3	+1.52, 1D9	Modulation of cellular proliferation through ion transport activity (Grzmil et al., 2004)
<i>2610204L23Rik</i>	+1.36, 3E3	Unknown function
<i>Itm1</i> , integral membrane protein 1	+1.20, 3E3	Not reported (Chavan et al., 2003) <sup>c</sup>
<i>Nfe2l1</i> , nuclear factor erythroid derived 2-like 1	+1.19, 3E3	Not reported (Farmer et al., 1997) <sup>d</sup>
<i>Itgb1</i> , integrin, beta 1	+1.13, 3E3	Initiation and maintenance of in vivo tumor growth (White et al., 2004)
<i>Sdc1</i> , syndecan 1	+1.08, 1D3	Involvement in cellular proliferation, migration and cell-matrix interactions (Alexander et al., 2000)

\*Gene ontology Tier 2, molecular component “extracellular” gene list was extracted from mAdb (<http://nciarray.nci.nih.gov/>) with a O/E (observed/expected by chance) index of 2.03 for the statistically significant data subset respective to the complete dataset.

<sup>a</sup>Data analysis as described in Table 1.

<sup>b</sup>Probably involved in cell differentiation and proliferation during inner ear embryogenesis.

<sup>c</sup>Involved in protein kinase C-mediated glycosilation in yeast.

<sup>d</sup>Essential for embryonic development.

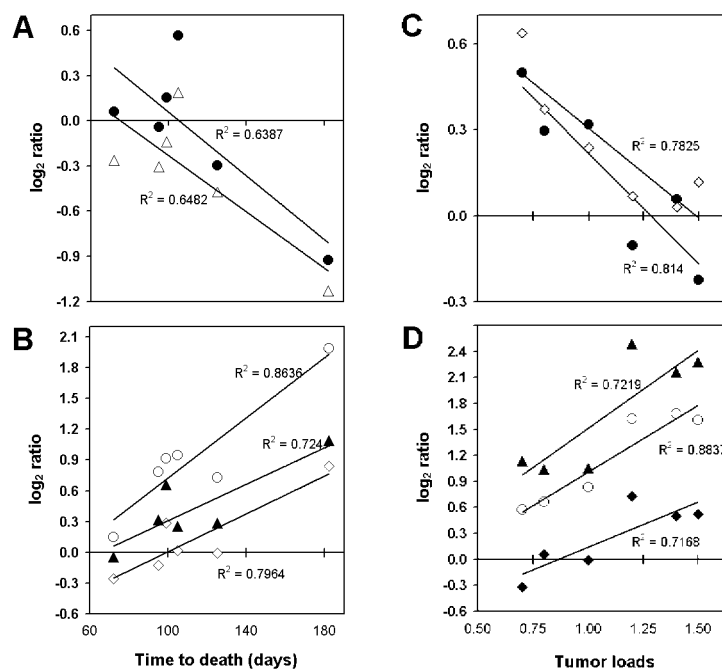


Fig. 3. Correlation of microarray results with in vivo tumorigenic parameters. Tumorigenic data was extracted from Roby et al. (2000). Replicate microarray results were correlated with time to death (A, B) and tumor loads (C, D) as class labels using the tool Pomelo (<http://pomelo.bioinfo.cnio.es/>). Symbols in charts A and B are: Pura (●),

5730469M10Rik (△), BC021790 (○), Cnn3 (▲) and clone H3111F06 (◇). Symbols in charts C and D are: Map4k4 (◇), Crsp2 (●), Tgfb1i4 (▲), Arpc1b (○) and 2310016E02Rik (◆).  $R^2$  values are shown close to its corresponding tendency line.

and IF5 with the following 4 types of human ovarian tumors: serous borderline ovarian tumor (sBOT), mucinous borderline ovarian tumor (mBOT), low malignant potential tumor (LMPT), and ovarian carcinoma stage III. After pre-processing of both datasets, we matched mouse-human gene symbols. Upon SOM analysis, the clusters in Figure 4A and B showed the best mouse-human similarity in upregulated and downregulated genes, respectively. The highest resemblance was with human sBOT and mBOT (upregulated) and with human LMPT (downregulated). Then, each group was analyzed with the tool FatiGO for “biological process,” level 3. As depicted in Figure 4C, “metabolism,” “cell growth and/or maintenance,” “cell communication,” and “response to external stimulus” were the highest represented biological functions in matched mouse-human patterns of gene expression. These results support previous findings of our group at the level of genomic imbalances similar between MOSE chromosomes 19, 15, 8, 7, 5, and 4 and its corresponding syntenic fragments of human chromosomes found in ovarian malignancies of epithelial origin including LMPT, serous carcinoma, and carcinoma cell lines (Urzúa et al., 2005).

## DISCUSSION

Aberrations in the wound repair of ovarian surface following repetitive ovulation are linked to the etiology of ovarian cancer (Purdie et al., 2003). This mouse cancer model was established by isolation and continuous culture of ovarian surface epithelial cells. During this process, MOSE cells underwent transformation and acquired tumorigenic ability (Roby et al., 2000). As shown in Table 1, 10 from the top 20 differentially expressed genes are involved in human ovarian cancer: (1) osteopontin (*Spp1*) is a calcium-binding, secreted glyco-phosphoprotein implicated in tumor progression and metastasis (Wai and Kuo, 2004), and postulated as ovarian cancer marker (Kim et al., 2002; Brakora et al.,

2004); (2) the cytochrome *Cyp1b1* oxidizes structurally unrelated compounds, including steroids, fatty acids, and xenobiotics. Confers drug resistance and it was detected in 92% and 94% of primary and metastatic ovarian cancers, respectively (McFadyen et al., 2001); (3) *Btg1* (B-cell translocation gene), originally described as an antiproliferative gene (Rouault et al., 1992), has recently been involved in endothelial cell angiogenesis and migration (Iwai et al., 2004). Interestingly, the *Btg1* protein was identified in pleural effusions of a patient affected by ovarian cancer (Bard et al., 2004); (4) The complement inhibitor factor H (Cfh) is secreted by ovarian tumor cells as a complement resistance mechanism to evade immune attack (Junnikkala et al., 2002); (5–6) Metallothioneins 1 and 2 (*Mt1*, *Mt2*) participate in cell proliferation, protection from oxidative stress, and multi-drug resistance in human cancers. *Mt* expression correlates with histological grade of ovarian carcinomas, whereas the product of glutathione per *Mt1*-*Mt2* protein levels is negatively associated with survival of grade I carcinomas (Hengstler et al., 2001); (7) A role for the IGF/insulin system in epithelial ovarian cancer has been proposed (Kalli and Conover, 2003), although *Igfbp5* was rarely expressed in four human ovarian carcinoma cell lines (Hofmann et al., 1994). This observation agrees with downregulation of this gene in all MOSE cells; (8–9) *Gstm1* and *Gstm2* catalyze the conjugation of glutathione to potentially genotoxic compounds. The *Gstm1*-null plus *Gstm2*-null combination is associated with unresponsiveness to primary chemotherapy in ovarian cancer patients (Howells et al., 1998). The biological effect of a null genotype would be functionally equivalent to downregulate its expression. This is precisely we observed in MOSE cells. However, a positive correlation has been reported between *GST*-*mu* expression and the malignant status of ovarian tumors (Matsumoto et al., 1997); (10) Breakpoints flanking the *ESR1* gene, a transcription factor involved in hormone-

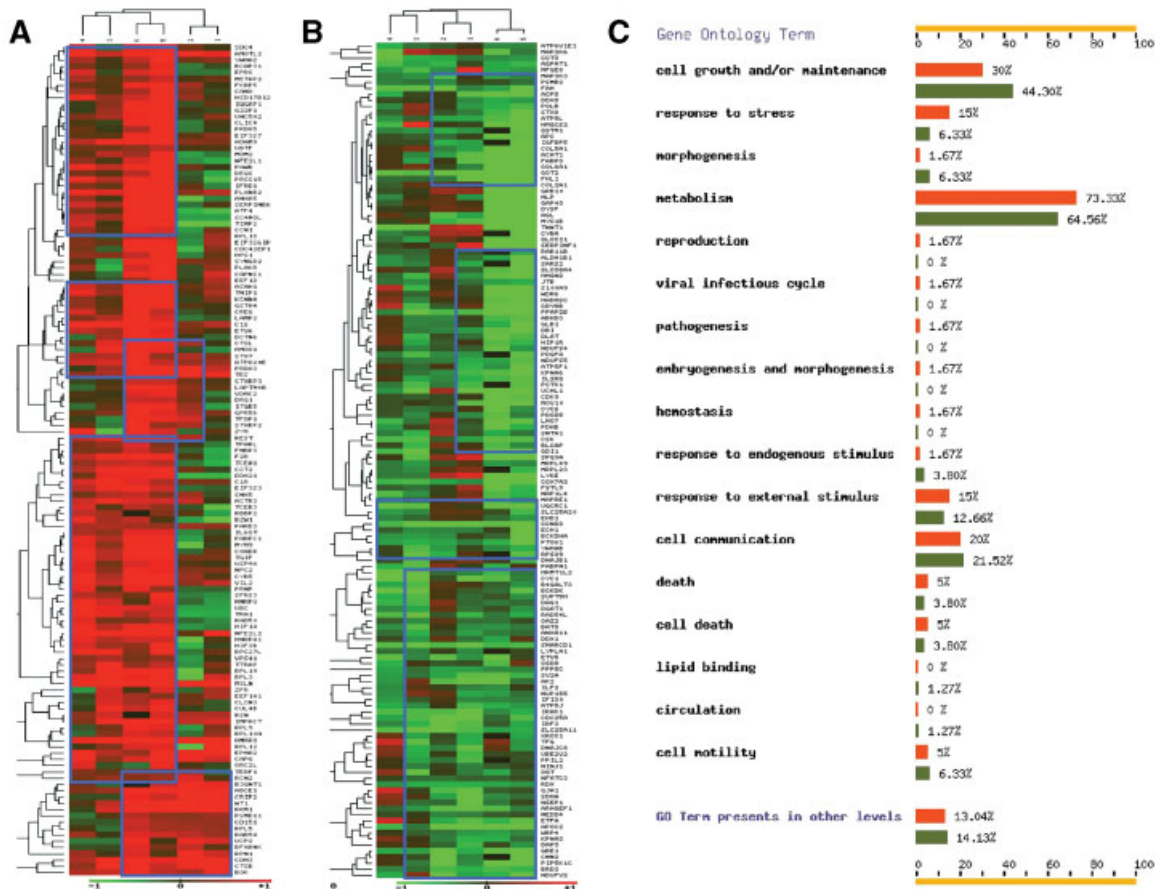


Fig. 4. Partial mouse-human comparison of ovarian gene expression. Expression ratios of human ovarian tumors (1=Low malignant potential tumor; 2=Ovarian carcinoma stage III; 3=Serous borderline ovarian tumor; 4=Mucinous borderline ovarian tumor), and MOSE cell lines (5=IG10; 6=IF5) were matched for 872 annotated genes showing identical gene symbol and equivalent biological function. Self-organizing map analysis (SOM) and clustering was

done with GEPAS (<http://gepas.bioinfo.cnio.es/tools.html>) under rectangular topology and 3,2-X,Y map dimensions. Maximal resemblance between mouse-human upregulated (cluster A) and downregulated (cluster B) gene expression is highlighted with blue squares. These genes were selected for further Gene Ontology datamining using the FatiGO tool (part C).

mediated gene repression, were identified in 39–76% of ovarian carcinomas (Hansen et al., 2002).

### Alterations of signaling and metabolic pathways

Altered pathways in MOSE cells are summarized in Table 3. An essential role of the MAPK cascade in proliferation, survival, and apoptosis of ovarian neoplastic cells has been proposed (Choi et al., 2003). Members of this pathway are the heat shock proteins *Hspb1*, *Hspb5*, and the oncogen *myc*. The activity of *myc* could be linked to *Pura*, a transcription activator that binds to the *c-myc* promoter, based on the correlation of *Pura* with “time to death” (Fig. 3A). *Ras*, another oncogen of the MAPK pathway involved in ovarian carcinoma, may be physiologically active in MOSE cells, via downregulation of *Rasa1*, whose normal role is to inhibit *Ras* (Rebhan et al., 1997).

Besides its function in apoptosis suppression, *Chuk* is involved in the chemotherapeutic response of human tumor ovarian cells (Huang and Fan, 2002) and we show here to be over-expressed in MOSE cells. Finally, a role in neoplastic transformation in various malignancies-including ovarian cancer- has been attributed to *Jak2*, a non-receptor tyrosine kinase involved in cytokine signaling (Verma et al., 2003). The interaction of *Ptpre* (receptor-type protein tyrosine phosphatase epsilon) with the *Jak-STAT* pathway is proposed as this protein

in vitro inhibits apoptosis in IL-6 stimulated murine M1 leukemic cells (Tanuma et al., 2000). Production of IL-6 is an attribute of ovarian cancer cells (Toutirais et al., 2003).

Anomalous *GST* expression is involved in chemotherapy resistance (Balendiran et al., 2004). Because not all drugs are conjugated with glutathione or are *GST* substrates for catalysis, a novel role for *GSTs* has emerged in regulating the MAPK pathway (Townsend and Tew, 2003). The expression of *Gstm1*, *Gstm2*, and *Gstm6* were downregulated in MOSE cells, whereas *Gsto1* was over-expressed. *Gsto1* is also located in mouse chromosome 19. In addition, *Gpx1* downregulation promotes malignant transformation through impairing the cellular ability to counteract oxidative DNA damage (Diwadkar-Navsariwala and Diamond, 2004).

Aiming to generate precursors for de novo nucleotide synthesis, tumor cells often have an abnormally high glycolytic flux (Warburg et al., 1924). Accordingly, *Gapd* and *Pgk1*, which catalyze two consecutive reactions leading to ATP synthesis in glycolysis, were upregulated in MOSE cells. The roles of *Pgk1* and *Gapd* in ovarian cancer and the function of *Eno1*, another glycolytic gene, in lung tumorigenesis are shown in Table 3.

### Cytoskeletal proteins

*Pcdh7*, *Dsg2* and *Iqgap1* were upregulated in all MOSE cells. *Pcdh7* is a cadherin-related neuronal



TABLE 3. Pathways selectively altered in MOSE cells

Pathway <sup>a</sup>	Genes <sup>b</sup>	Roles in ovarian tumorigenesis
MAPK signaling (Choi et al., 2003)	<b>Hpsb1</b>	Expressed in malignant ovarian epithelial tumors (Elpek et al., 2003). Independent prognosis and ovarian cancer survival indicator after 5-years (Geisler et al., 2004). Downregulated by paclitaxel in BG-1 ovarian tumor cells (Tanaka et al., 2004)
	<b>c-myc</b>	Frequently amplified in ovarian cancer (Baker et al., 1990). C-myc expression is related to chemotherapy response. Putative ovarian cancer prognostic factor (Iba et al., 2004)
	<b>Rac1</b> <b>Chuk</b>	Migration signaling of ovarian tumor cells (Bourguignon et al., 2001) Regulates paclitaxel induced apoptosis in ovarian cancer OV2008 cell line (Huang and Fan, 2002)
	<b>Rasa1</b>	Negative modulation of Ras activity (Rebhan et al., 1997)
Glutathione metabolism (Townsend and Tew, 2003)	<i>Gstm1, Gstm2, Gstm6</i>	Chemotherapy resistance and poor prognosis of solid tumors (Balendiran et al., 2004)
	<i>Gsto1</i>	Enhances drug resistance through recycling of oxidized ascorbic acid (Bode et al., 1999)
Glycolysis/gluconeogenesis (Gatenby and Gillies, 2004)	<i>Gpx1</i> <b>Pgk1</b>	Oxidative stress protection (Diwadkar-Navsariwala and Diamond, 2004) Overexpression induces a multidrug resistance in the human ovarian cancer cell line SW626TR (Duan et al., 2002)
	<b>Gapd</b>	Binds to the 3'-UTR region of CSF-1 mRNA promoting metastasis in ovarian tumor cells (Bonafe et al., 2005)
	<i>Eno1</i> <b>Jak2</b>	Downregulation plays a role in non-small cell lung cancer (Chang et al., 2003). Constitutively expressed in mutant-p53 ovarian cancer cells (Reid et al., 2004). Indirect cisplatin target in ovarian cancer and sarcoma cells (Song et al., 2004)
Jak-STAT (Verma et al., 2003)	<i>Ptprc</i> <sup>c</sup>	Inhibit apoptosis in IL-6 stimulated murine M1 leukemic cells (Tanuma et al., 2000)

<sup>a</sup>Obtained from KEGG pathways database (available at <http://www.genome.jp/kegg/pathway.html>). A key reference is indicated between parentheses.

<sup>b</sup>Gene symbols in bold correspond to genes reported to be involved in ovarian cancer as supported by relevant literature.

<sup>c</sup>Function inferred from literature, not appearing in the KEGG database.

receptor involved in calcium dependent cell–cell adhesion. Dsg2 shares similar features and forms desmosomal junctions and intermediate filaments (Chitaev and Troyanovsky, 1997). Cell lines established from human ovarian serous adenocarcinoma exhibit tonofilaments and desmosomes (Yamada et al., 1999), which may still be functional in tumor cells because Dsg2 is upregulated in squamous cell skin carcinoma showing positive correlation with metastasis (Kurzen et al., 2003). Iqgap1, a scaffolding protein involved in cell migration, has found to act as a signaling integrator of Cdc42 cytoskeletal function and CD44-ERalpha “cross-talk” during ovarian cancer progression (Bourguignon et al., 2005).

Downregulated genes included *Homer2*, a postsynaptic scaffolding protein that interconnects glutamate receptors with actin-cytoskeleton and Rho-(Cdc42) (Shiraishi et al., 1999). *Spnb2* ( $\beta$ -spectrin 2) interacts with calmodulin in a calcium-dependent manner thus participating in movement of cytoskeleton at the membrane (Rebhan et al., 1997). *Col6a1* (collagen type VI, alpha 1) is an extracellular cell binding protein whose deficiency modifies fibronectin organization in the extracellular matrix of fibroblasts (Sabatelli et al., 2001) and promote apoptosis and mitochondrial dysfunction in *Col6a1* null mice (Irwin et al., 2003).

#### Genes correlated to tumorigenesis

As cited before, *Pura* was negatively correlated with “time to death” (Fig. 3A), a finding apparently opposed to its putative role as tumor suppressor-like gene in myeloid leukemic (Ulger et al., 2003) and glioblastoma cells (Darbinian et al., 2001). Interestingly, the gene *5730469M10Rik* that codes for a hypothetical protein, exhibited identical correlation. In contrast, *Cnn3* (calponin 3, acidic) exhibited the opposite behavior. *Cnn3* is a thin filament-associated protein implicated in regulation of smooth muscle contraction. It has recently shown to stabilize the actin cytoskeleton thus inhibiting metastatic capacity of melanoma and adenocarcinoma

cells (Lener et al., 2004). Regarding “tumor loads” analysis (Fig. 3C–D), both *Crsp2*, a cofactor required for Sp1 transcriptional activation, and *Map4k4*, a ser/thr kinase that acts in response to environmental stress and cytokines, showed negative correlation. *Map4k4* is highly expressed in many tumor cell lines and modulates transformation, adhesion and invasion (Wright et al., 2003). On the other hand, *Arpc1b* (actin related protein 2/3 complex, subunit 1B), a protein involved in actin filaments organization was positively correlated to tumor loads, precisely opposed as detected in human gastric tumors (Kaneda et al., 2002).

In summary, despite the obvious mouse-human differences at the level of chromosomal organization, we have proven using DNA-microarray technology, that MOSE cells bear transcriptional alterations closely resembling human ovarian carcinomas. Signal transduction pathways, cell motility, and extracellular-secretable protein products are relevant in this model. Our findings may provide clues for the study and evaluation of a variety of novel tumor progression, therapeutic and diagnostic targets for this devastating disease.

#### ACKNOWLEDGMENTS

We thank Gary Owens for technical assistance, Casey Frankenberger and Xiaolin Wu for help with data analysis. Thanks to Paola Perez and Luisa Herrera for critical reading of the manuscript. U.U. was an exchange scientist supported by a fellowship from the Oncology Research Faculty Development Program, Office of International Affairs of the National Cancer Institute. This work has been funded in whole or in part with Federal Funds from the National Cancer Institute, National Institutes of Health under contract N01-CO-12400. The content of this publication does not necessarily reflect the view or policies of the Department of Health and Human Services, nor does mention of trade names, commercial products, or organizations imply endorsement by the U.S. government.

## LITERATURE CITED

- Adam GC, Sorenson EJ, Cravatt BF. 2002. Proteomic profiling of mechanistically distinct enzyme classes using a common chemotype. *Nat Biotechnol* 20:805–809.
- Alexander CM, Reichsman F, Hinkes MT, Lincecum J, Becker KA, Cumberledge S, Bernfield M. 2000. Syndecan-1 is required for Wnt-1-induced mammary tumorigenesis in mice. *Nat Genet* 25:329–332.
- American Cancer Society. 2004. Cancer Facts and Figures [Internet]. Available from: [http://www.cancer.org/downloads/STT/CAFF\\_finalPWSecured.pdf](http://www.cancer.org/downloads/STT/CAFF_finalPWSecured.pdf).
- Baker VV, Borst MP, Dixon D, Hatch KD, Shingleton HM, Miller D. 1990. c-myc amplification in ovarian cancer. *Gynecol Oncol* 38(3):340–342.
- Balendiran GK, Dabur R, Fraser D. 2004. The role of glutathione in cancer. *Cell Biochem Funct* 22(6):343–352.
- Bard MP, Hegmans JP, Hemmes A, Luider TM, Willemsen R, Severijnen LA, van Meerbeeck JP, Burgers SA, Hoogsteden HC, Lambrecht BN. 2004. Proteomic analysis of exosomes isolated from human malignant pleural effusions. *Am J Respir Cell Mol Biol* 31(1):114–121.
- Ben-Porath I, Yanuka O, Benvenisty N. 1999. The *tmp* gene, encoding a membrane protein, is a c-Myc target with a tumorigenic activity. *Mol Cell Biol* 19:3529–3539.
- Bode AM, Liang HQ, Green EH, Meyer TE, Buckley DJ, Norris A, Gout PW, Buckley AR. 1999. Ascorbic acid recycling in Nb2 lymphoma cells: Implications for tumor progression. *Free Radic Biol Med* 26(1–2):136–147.
- Bonafe N, Gilmore-Hebert M, Folk NL, Azodi M, Zhou Y, Chambers SK. 2005. Glycerolaldehyde-3-phosphate dehydrogenase binds to the AU-Rich 3' untranslated region of colony-stimulating factor-1 (CSF-1) messenger RNA in human ovarian cancer cells: Possible role in CSF-1 posttranscriptional regulation and tumor phenotype. *Cancer Res* 65(9):3762–3771.
- Bourguignon LY, Zhu H, Zhou B, Diedrich F, Singleton PA, Hung MC. 2001. Hyaluronan promotes CD44v3-Vav2 interaction with Grb2-p185(HER2) and induces Rac1 and Ras signaling during ovarian tumor cell migration and growth. *J Biol Chem* 276(52):48679–48692.
- Bourguignon LY, Gilad E, Rothman K, Peyrollier K. 2005. Hyaluronan-CD44 interaction with IQGAP1 promotes Cdc42 and ERK signaling, leading to actin binding, Elk-1/estrogen receptor transcriptional activation, and ovarian cancer progression. *J Biol Chem* 280(12):11961–11972.
- Brakora KA, Lee H, Yusuf R, Sullivan L, Harris A, Colella T, Seiden MV. 2004. Utility of osteopontin as a biomarker in recurrent epithelial ovarian cancer. *Gynecol Oncol* 93(2):361–365.
- Chang YS, Wu W, Walsh G, Hong WK, Mao L. 2003. Enolase-alpha is frequently down-regulated in non-small cell lung cancer and predicts aggressive biological behavior. *Clin Cancer Res* 9(10 Pt 1):3641–3644.
- Chavan M, Rekowicz M, Lennarz W. 2003. Insight into functional aspects of Stt3p, a subunit of the oligosaccharyl transferase. Evidence for interaction of the N-terminal domain of Stt3p with the protein kinase C cascade. *J Biol Chem* 278:51441–51447.
- Chitavev NA, Troyanovsky SM. 1997. Direct Ca<sup>2+</sup>-dependent heterophilic interaction between desmosomal cadherins, desmoglein and desmocollin, contributes to cell-cell adhesion. *J Cell Biol* 138(1):193–201.
- Choi KC, Auersperg N, Leung PC. 2003. Mitogen-activated protein kinases in normal and (pre)neoplastic ovarian surface epithelium. *Reprod Biol Endocrinol* 1(1):71.
- Coppola D, Szabo M, Boulware D, Muraca P, Alsarraj M, Chambers AF, Yeatman TJ. 2004. Correlation of osteopontin protein expression and pathological stage across a wide variety of tumor histologies. *Clin Cancer Res* 10:184–190.
- Darbinian N, Gallia GL, King J, Del Valle L, Johnson EM, Khalili K. 2001. Growth inhibition of glioblastoma cells by human Pur(alpha). *J Cell Physiol* 189(3):334–340.
- Di Pietro E, Wang XL, MacKenzie RE. 2004. The expression of mitochondrial methylenetetrahydrofolate dehydrogenase-cyclohydrolase supports a role in rapid cell growth. *Biochim Biophys Acta* 1674:78–84.
- Diwadkar-Navsariwala V, Diamond AM. 2004. The link between selenium and chemoprevention: A case for selenoproteins. *J Nutr* 134(11):2899–2902.
- Donin N, et al. 2003. Complement resistance of human carcinoma cells depends on membrane regulatory proteins, protein kinases and sialic acid. *Clin Exp Immunol* 131(2):254–263.
- Duan Z, Lamendola DE, Yusuf RZ, Penson RT, Preffer FI, Seiden MV. 2002. Overexpression of human phosphoglycerate kinase 1 (PGK1) induces a multidrug resistance phenotype. *Anticancer Res* 22(4):1933–1941.
- Elpek GO, Karaveli S, Simsek T, Keles N, Aksoy NH. 2003. Expression of heat-shock proteins hsp27, hsp70 and hsp90 in malignant epithelial tumour of the ovaries. *APMIS* 111(4):523–530.
- Farmer SC, Sun CW, Winnier GE, Hogan BL, Townes TM. 1997. The bZIP transcription factor LCR-F1 is essential for mesoderm formation in mouse development. *Genes Dev* 11:786–798.
- Gatenby RA, Gillies RJ. 2004. Why do cancers have high aerobic glycolysis? *Nat Rev Cancer* 4:891–899.
- Geisler JP, Tammela JE, Manahan KJ, Geisler HE, Miller GA, Zhou Z, Wiemann MC. 2004. HSP27 in patients with ovarian carcinoma: Still an independent prognostic indicator at 60 months follow-up. *Eur J Gynaecol Oncol* 25(2):165–168.
- Grzml M, Voigt S, Thelen P, Hemmerlein B, Helmke K, Burfeind P. 2004. Up-regulated expression of the MAT-8 gene in prostate cancer and its siRNA-mediated inhibition of expression induces a decrease in proliferation of human prostate carcinoma cells. *Int J Oncol* 24:97–105.
- Gu YC, Nilsson K, Eng H, Ekblom M. 2000. Association of extracellular matrix proteins fibulin-1 and fibulin-2 with fibronectin in bone marrow stroma. *Br J Haematol* 109:305–313.
- Hansen LL, Jensen LL, Dimitrakakis C, Michalas S, Gilbert F, Barber HR, Overgaard J, Arzimanoglou II. 2002. Allelic imbalance in selected chromosomal regions in ovarian cancer. *Cancer Genet Cytogenet* 139(1):1–8.
- Hengstler JG, Pilch H, Schmidt M, Dahlenburg H, Sagemuller J, Schiffer I, Oesch F, Knapstein PG, Kaina B, Tanner B. 2001. Metallothionein expression in ovarian cancer in relation to histopathological parameters and molecular markers of prognosis. *Int J Cancer* 95(2):121–127.
- Herrero J, Diaz-Uriarte R, Dopazo J. 2003. Gene expression data preprocessing. *Bioinformatics* 19:655–656.
- Herrero J, Vaquerizas JM, Al-Shahrour F, Conde L, Mateos A, Diaz-Uriarte JS, Dopazo J. 2004. New challenges in gene expression data analysis and the extended GEPAS. *Nucleic Acids Res* 32 (Web Server issue):W485–W491.
- Hildebrandt T, Preiherr J, Tarbe N, Klostermann S, Van Muijen GN, Weidle UH. 2000. Identification of THW, a putative new tumor suppressor gene. *Anticancer Res* 20:2801–2809.
- Hofmann J, Wegmann B, Hackenberg R, Kunzmann R, Schulz KD, Havemann K. 1994. Production of insulin-like growth factor binding proteins by human ovarian carcinoma cells. *J Cancer Res Clin Oncol* 120(3):137–142.
- Howells RE, Redman CW, Dhar KK, Sarhanis P, Musgrove C, Jones PW, Alldersea J, Fryer AA, Hoban PR, Strange RC. 1998. Association of glutathione S-transferase GSTM1 and GSTT1 null genotypes with clinical outcome in epithelial ovarian cancer. *Clin Cancer Res* 4(10):2439–2445.
- Huang Y, Fan W. 2002. IkappaB kinase activation is involved in regulation of paclitaxel-induced apoptosis in human tumor cell lines. *Mol Pharmacol* 61(1):105–113.
- Iba T, Kigawa J, Kanamori Y, Itamochi H, Oishi T, Simada M, Uegaki K, Naniwa J, Terakawa N. 2004. Expression of the c-myc gene as a predictor of chemotherapy response and a prognostic factor in patients with ovarian cancer. *Cancer Sci* 95(5):418–423.
- Ihrig RA, Reczek E, Horner JS, Khachatrian L, Sage J, Jacks T, Attardi LD. 2003. Perp is a mediator of p53-dependent apoptosis in diverse cell types. *Curr Biol* 13:1985–1990.
- Iovanna JL. 2002. Expression of the stress-associated protein p8 is a requisite for tumor development. *Int J Gastrointest Cancer* 31:89–98.
- Irwin WA, Bergamin N, Sabatelli P, Reggiani C, Meghian A, Merlini L, Braghetta P, Columbaro M, Volpin D, Bressan GM, Bernardi P, Bonaldo P. 2003. Mitochondrial dysfunction and apoptosis in myopathic mice with collagen VI deficiency. *Nat Genet* 35(4):367–371.
- Iwai K, Hirata K, Ishida T, Takeuchi S, Hirase T, Rikitake Y, Kojima Y, Inoue N, Kawashima S, Yokoyama M. 2004. An anti-proliferative gene BTG1 regulates angiogenesis in vitro. *Biochem Biophys Res Commun* 316(3):628–635.
- Junnikkala S, Hakulinen J, Jarva H, Manuelian T, Bjorge L, Butzow R, Zipfel PF, Meri S. 2002. Secretion of soluble complement inhibitors factor H and factor H-like protein (FHL-1) by ovarian tumour cells. *Br J Cancer* 87(10):1119–1127.
- Kalli KR, Conover CA. 2003. The insulin-like growth factor/insulin system in epithelial ovarian cancer. *Front Biosci* 8:d714–d722.
- Kaneda A, Kaminishi M, Nakanishi Y, Sugimura T, Ushijima T. 2002. Reduced expression of the insulin-induced protein 1 and p41 Arp2/3 complex genes in human gastric cancers. *Int J Cancer* 100(1):57–62.
- Kim JH, Skates SJ, Ueda T, Wong K, Schorge JO, Feltmate CM, Berkowitz RS, Cramer DW, Mok SC. 2002. Osteopontin as a potential diagnostic biomarker for ovarian cancer. *JAMA* 287(13):1671–1679.
- King JA, Ofori-Acquah SF, Stevens T, Al-Mehdi AB, Fodstad O, Jiang WG. 2004. Activated leukocyte cell adhesion molecule in breast cancer: Prognostic indicator. *Breast Cancer Res* 6:R478–R487.
- Kobayashi M, Kinouchi T, Hakamata Y, Kamiakito T, Kuriki K, Suzuki K, Tokue A, Fukayama M, Tanaka A. 2001. Isolation of an androgen-inducible novel lipocalin gene, Arg1, from androgen-dependent mouse mammary Shionogi carcinoma cells. *J Steroid Biochem Mol Biol* 77:109–115.
- Kurzen H, Münzing I, Hartschuh W. 2003. Expression of desmosomal proteins in squamous cell carcinomas of the skin. *J Cutan Pathol* 30(10):621–630.
- Lener T, Burgstaller G, Gimona M. 2004. The role of calponin in the gene profile of metastatic cells: Inhibition of metastatic cell motility by multiple calponin repeats. *FEBS Lett* 556(1–3):221–226.
- Marin A, Lopez de Cerain A, Hamilton E, Lewis AD, Martinez-Penuela JM, Idoate MA, Bello J. 1997. DT-diaphorase and cytochrome B5 reductase in human lung and breast tumours. *Br J Cancer* 76:923–929.
- Matsumoto T, Hayase R, Kodama J, Kamimura S, Yoshinouchi M, Kudo T. 1997. Immunohistochemical analysis of glutathione S-transferase mu expression in ovarian tumors. *Eur J Obstet Gynecol Reprod Biol* 73(2):171–176.
- McFadyen MC, Cruickshank ME, Miller ID, McLeod HL, Melvin WT, Haites NE, Parkin D, Murray GI. 2001. Cytochrome P450 CYP1B1 over-expression in primary and metastatic ovarian cancer. *Br J Cancer* 85(2):242–246.
- Murray GI, Melvin WT, Greenlee WF, Burke MD. 2001. Regulation, function, and tissue-specific expression of cytochrome P450 CYP1B1. *Ann Rev Pharmacol Toxicol* 41:297–316.
- Pilipenko VV, Reece A, Choo DI, Greinwald JH. 2004. Genomic organization and expression analysis of the murine Fam3c gene. *Gene* 335:159–168.
- Purdie DM, Bain CJ, Siskind V, Webb PM, Green AC. 2003. Ovulation and risk of epithelial ovarian cancer. *Int J Cancer* 104(2):228–232.
- Rebhan M, Chalifa-Caspi V, Prilusky J, Lancet D. 1997. GeneCards: Encyclopedia for genes, proteins and diseases. Weizmann Institute of Science, Bioinformatics Unit and Genome Center (Rehovot, Israel), 1997. [Update 2.30u1, September 6th, 2004].
- Reid T, Jin X, Song H, Tang HJ, Reynolds RK, Lin J. 2004. Modulation of Janus kinase 2 by p53 in ovarian cancer cells. *Biochem Biophys Res Commun* 321(2):441–447.
- Roby KF, Taylor CC, Sweetwood JP, Cheng Y, Pace JL, Tawfik O, Persons DL, Smith PG, Terranova PF. 2000. Development of a syngeneic mouse model for events related to ovarian cancer. *Carcinogenesis* 21:585–591.
- Rouault JP, Rimokh R, Tessa C, Paranhos G, French M, Duret L, Garocchio M, Germain D, Samarut J, Magaud JP. 1992. BTG1, a member of a new family of anti-proliferative genes. *EMBO J* 11(4):1663–1670.
- Sabatelli P, Bonaldo P, Lattanzi G, Braghetta P, Bergamin N, Capanni C, Mattioli E, Columbaro M, Ognibene A, Pepe G, Bertini E, Merlini L, Maraldi NM, Squarzone S. 2001. Collagen VI deficiency affects the organization of fibronectin in the extracellular matrix of cultured fibroblasts. *Matrix Biol* 20(7):475–486.
- Sausville EA. 2002. Complexities in the development of cyclin-dependent kinase inhibitor drugs. *Trends Mol Med* 8(4 Suppl):S32–S37.
- Seth P, Porter D, Lahti-Domenici J, Geng Y, Richardson A, Polyak K. 2002. Cellular and molecular targets of estrogen in normal human breast tissue. *Cancer Res* 62:4540–4544.
- Sherman-Baust CA, Weeratna AT, Rangel LB, Pizer ES, Cho KR, Schwartz DR, Shock T, Morin PJ. 2003. Remodeling of the extracellular matrix through



- overexpression of collagen VI contributes to cisplatin resistance in ovarian cancer cells. *Cancer Cell* 3:377–386.
- Shiraishi Y, Mizutani A, Bito H, Fujisawa K, Narumiya S, Mikoshiba K, Furuichi T. 1999. Cupidin, an isoform of Homer/Vesl, interacts with the actin cytoskeleton and activated rho family small GTPases and is expressed in developing mouse cerebellar granule cells. *J Neurosci* 19(19):8389–8400.
- Song H, Sondak VK, Barber DL, Reid TJ, Lin J. 2004. Modulation of Janus kinase 2 by cisplatin in cancer cells. *Int J Oncol* 24(4):1017–1026.
- Steel LF, Shumpert D, Trotter M, Seeholzer SH, Evans AA, London WT, Dwek R, Block TM. 2003. A strategy for the comparative analysis of serum proteomes for the discovery of biomarkers for hepatocellular carcinoma. *Proteomics* 3:601–609.
- Tanaka Y, Fujiwara K, Tanaka H, Maehata K, Kohno I. 2004. Paclitaxel inhibits expression of heat shock protein 27 in ovarian and uterine cancer cells. *Int J Gynecol Cancer* 14(4):616–620.
- Tanuma N, Nakamura K, Shima H, Kikuchi K. 2000. Protein-tyrosine phosphatase PTPepsilon C inhibits Jak-STAT signaling and differentiation induced by interleukin-6 and leukemia inhibitory factor in M1 leukemia cells. *J Biol Chem* 275(36):28216–28221.
- Toutirais O, Chartier P, Dubois D, Bouet F, Leveque J, Catros-Quemener V, Genetet N. 2003. Constitutive expression of TGF-beta1, interleukin-6 and interleukin-8 by tumor cells as a major component of immune escape in human ovarian carcinoma. *Eur Cytokine Netw* 14(4):246–255.
- Townsend DM, Tew KD. 2003. The role of glutathione-S-transferase in anti-cancer drug resistance. *Oncogene* 22(47):7369–7375.
- Ulger C, Toruner GA, Alkan M, Mohammed M, Damani S, Kang J, Galante A, Aviv H, Soteropoulos P, Tolia PP, Schwalb MN, Dermody JJ. 2003. Comprehensive genome-wide comparison of DNA and RNA level scan using microarray technology for identification of candidate cancer-related genes in the HL-60 cell line. *Cancer Genet Cytogenet* 147(1):28–35.
- Urzúa U, Frankenberger C, Gangi L, Mayer S, Burkett S, Munroe D.J. 2005. Microarray comparative genomic hybridization profile of a murine model for epithelial ovarian cancer reveals genomic imbalances resembling human ovarian carcinomas. To appear in *Tumour Biol* 26:236–244.
- Vanderhyden BC, Shaw TJ, Ethier JF. 2003. Animal models of ovarian cancer. *Reprod Biol Endocrinol* 1(1):67.
- Vaquerizas JM, Dopazo J, Diaz-Uriarte R. 2004. DNMAID: Web-based diagnosis and normalization for microarray data. *Bioinformatics* 20:3656–3658.
- Verma A, Kambhampati S, Parmar S, Platanias LC. 2003. Jak family of kinases in cancer. *Cancer Metastasis Rev* 22(4):423–434.
- Wai PY, Kuo PC. 2004. The role of osteopontin in tumor metastasis. *J Surg Res* 121(2):228–241.
- Warburg O., Posener K., Negelein E. 1924. On the metabolism of cancer cells. *Biochem Z* 152:319–344.
- Webb DJ, Nguyen DH, Sankovic M, Gonias SL. 1999. The very low density lipoprotein receptor regulates urokinase receptor catabolism and breast cancer cell motility in vitro. *J Biol Chem* 274:7412–7420.
- White DE, Kurpios NA, Zuo D, Hassell JA, Blaess S, Mueller U, Muller WJ. 2004. Targeted disruption of beta1-integrin in a transgenic mouse model of human breast cancer reveals an essential role in mammary tumor induction. *Cancer Cell* 6:159–170.
- Wright JH, Wang X, Manning G, LaMere BJ, Le P, Zhu S, Khatry D, Flanagan PM, Buckley SD, Whyte DB, Howlett AR, Bischoff JR, Lipson KE, Jallal B. 2003. The STE20 kinase HGK is broadly expressed in human tumor cells and can modulate cellular transformation, invasion, and adhesion. *Mol Cell Biol* 23(6):2068–2082.
- Yamada K, Tachibana T, Hashimoto H, Suzuki K, Yanagida S, Endoh H, Kimura E, Yasuda M, Tanaka T, Ishikawa H. 1999. Establishment and characterization of cell lines derived from serous adenocarcinoma (JHOS-2) and clear cell adenocarcinoma (JHOC-5, JHOC-6) of human ovary. *Hum Cell* 12(3):131–138.
- Yamashita Y, Kumabe T, Cho YY, Watanabe M, Kawagishi J, Yoshimoto T, Fujino T, Kang MJ, Yamamoto TT. 2000. Fatty acid induced glioma cell growth is mediated by the acyl-CoA synthetase 5 gene located on chromosome 10q25.1-q25.2, a region frequently deleted in malignant gliomas. *Oncogene* 19:5919–5925.
- Yamazaki T, Hibi K, Takase T, Tezel E, Nakayama H, Kasai Y, Ito K, Akiyama S, Nagasaka T, Nakao A. 2002. PGP9.5 as a marker for invasive colorectal cancer. *Clin Cancer Res* 8:192–195.
- Zhang Z, DuBois RN. 2001. Detection of differentially expressed genes in human colon carcinoma cells treated with a selective COX-2 inhibitor. *Oncogene* 20(33):4450–4456.